LETTER

doi:10.1038/nature19351

Primitive Solar System materials and Earth share a common initial ^{142}Nd abundance

A. Bouvier[1] & M. Boyet[2]

The early evolution of planetesimals and planets can be constrained using variations in the abundance of neodymium-142 (^{142}Nd), which arise from the initial distribution of ^{142}Nd within the protoplanetary disk and the radioactive decay of the short-lived samarium-146 isotope (^{146}Sm)[1,2]. The apparent offset in ^{142}Nd abundance found previously between chondritic meteorites and Earth[1,2] has been interpreted either as a possible consequence of nucleosynthetic variations within the protoplanetary disk[2–4] or as a function of the differentiation of Earth very early in its history[5]. Here we report high-precision Sm and Nd stable and radiogenic isotopic compositions of four calcium–aluminium-rich refractory inclusions (CAIs) from three CV-type carbonaceous chondrites, and of three whole-rock samples of unequilibrated enstatite chondrites. The CAIs, which are the first solids formed by condensation from the nebular gas, provide the best constraints for the isotopic evolution of the early Solar System. Using the mineral isochron method for individual CAIs, we find that CAIs without isotopic anomalies in Nd compared to the terrestrial composition share a ^{146}Sm/^{144}Sm–^{142}Nd/^{144}Nd isotopic evolution with Earth. The average ^{142}Nd/^{144}Nd composition for pristine enstatite chondrites that we calculate coincides with that of the accessible silicate layers of Earth. This relationship between CAIs, enstatite chondrites and Earth can only be a result of Earth having inherited the same initial abundance of ^{142}Nd and chondritic proportions of Sm and Nd. Consequently, ^{142}Nd isotopic heterogeneities found in other CAIs and among chondrite groups may arise from extrasolar grains that were present in the disk and incorporated in different proportions into these planetary objects. Our finding supports a chondritic Sm/Nd ratio for the bulk silicate Earth and, as a consequence, chondritic abundances for other refractory elements. It also removes the need for a hidden reservoir or for collisional erosion scenarios[5,6] to explain the ^{142}Nd/^{144}Nd composition of Earth.

The ^{146}Sm–^{142}Nd short-lived radiometric pair records the first few hundred million years (Myr) of the Solar System and provides a powerful geochemical tool for tracing the early silicate differentiation of planetary objects. However, its use as a precise chronometer has become more problematic in the past few years, owing to uncertainties in the half-life of ^{146}Sm (ref. 7), in the initial abundance of ^{146}Sm (ref. 8) and in the bulk Sm/Nd ratios of planetary bodies[9]. In addition, ^{142}Nd/^{144}Nd ratios in chondrites deviate by up to −40 p.p.m. from the terrestrial value[2–4], and model ^{146}Sm/^{144}Nd–^{142}Nd/^{144}Nd ages for silicate differentiation depend on the initial ^{142}Nd/^{144}Nd composition of the planets from which internal reservoirs subsequently evolved. The deviations of sample compositions from the Nd isotopic standard (and similarly for Sm normalized to ^{152}Sm) for a given isotope of mass i are expressed (in parts per million) as $\mu^i\mathrm{Nd} = [(^i\mathrm{Nd}/^{144}\mathrm{Nd})_{\mathrm{sample}}/(^i\mathrm{Nd}/^{144}\mathrm{Nd})_{\mathrm{reference}} - 1] \times 10^6$.

Isotopic measurements of planetary materials suggest that the solar nebula was not completely homogenized during the period of planetary accretion[10]. Large isotope anomalies have been detected at the microscale for presolar grains[11], and smaller anomalies are found for many refractory elements at the whole-rock scale (for example, Cr, Ti (ref. 12), Sr (ref. 13), Sm and Nd (ref. 3)). Among the different chondrite groups, the carbonaceous chondrites have stable isotopic compositions for several refractory elements furthest from the

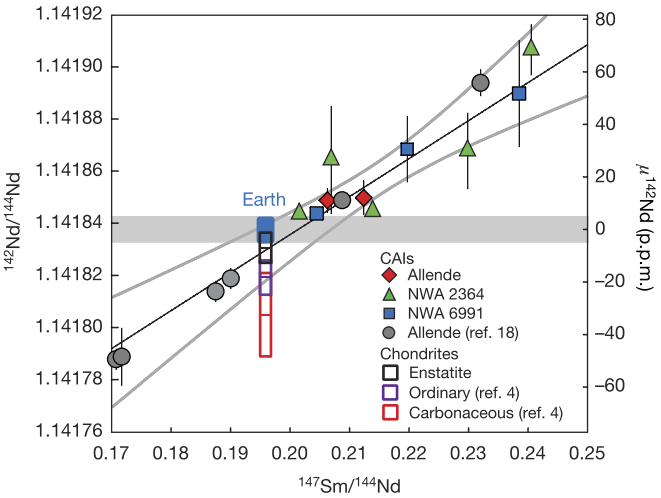

Figure 1 | ^{146}Sm–^{142}Nd mineral and bulk isochron of the Allende, NWA 2364 and NWA 6991 CAIs compared with the Allende Al3S4 CAI, the modern terrestrial composition and bulk-rock chondrite averages for enstatite, ordinary and carbonaceous chondrites. The data for Allende Al3S4 CAI are from ref. 18 and those for ordinary and carbonaceous chondrites are from ref. 4; all other data are from this study. The modern terrestrial composition is indicated by the blue rectangle labelled Earth, and is also represented by the grey band for the average ^{142}Nd/^{144}Nd ratio, which corresponds to μ^{142}Nd of the JNdi-1 standard (0 ± 5 p.p.m.; 2 s.d.). Regressions of NWA 6991 (black line) and NWA 2364 (not shown) yield ^{146}Sm/^{144}Sm ratios of 0.0072 ± 0.0024 (MSWD = 0.76) and 0.0069 ± 0.0056 (MSWD = 2.8), respectively, at the age of Sm–Nd isotopic closure. Considering data from all CAIs from this study, the slope of the regression line (not shown) is 0.0073 ± 0.0022 (MSWD = 3.3). The NWA 6991 CAI does not have any stable isotopic variations in Nd relative to Earth, removing the need for potential corrections from nucleosynthetic or neutron capture effects. The internal isochron regression of NWA 6991 (black line; grey lines indicate the 95% confidence interval) intersects the ^{142}Nd/^{144}Nd compositions of Earth and enstatite chondrites at a common ^{147}Sm/^{144}Nd ratio, which we find matches the chondritic ratio of 0.196 (ref. 27). All errors bars are two standard errors (2 s.e.) for individual data points. Respective means and errors for chondrite groups are given in the text; those for samples and standards from this study are provided in Supplementary Table 1. The left y axis shows the ^{142}Nd/^{144}Nd ratios; the right y axis shows the μ^{142}Nd values (in parts per million; deviation relative to the mean obtained on the JNdi-1 terrestrial standard). The heights of the rectangles for the chondrite groups indicate 2 s.d. on the μ^{142}Nd averages (horizontal bars); the widths indicate 2 s.e. on the CHUR ^{147}Sm/^{144}Nd ratio[27].

[1]University of Western Ontario, Department of Earth Sciences, Centre for Planetary Science and Exploration, London, Ontario N6A 3K7, Canada. [2]Clermont Université, Université Blaise Pascal, Laboratoire Magmas et Volcans, UMR CNRS 6524, Campus Universitaire des Cézeaux, 6 avenue Blaise Pascal, 63178 Aubière Cedex, France.

terrestrial composition, and so must constitute a small mass fraction of Earth's building blocks[14]. The enstatite chondrites and a few ungrouped chondrites and achondrite meteorites are the only meteorite groups so far that share identical oxygen isotopic compositions[15] with Earth and the Moon, suggesting a common reservoir for their accretion. The ordinary chondrites have an average $^{142}Nd/^{144}Nd$ deficit of -19 ± 5 p.p.m. (where the error indicates 2 standard deviations (s.d.); ref. 4) relative to modern terrestrial samples, whereas $^{142}Nd/^{144}Nd$ ratios in enstatite chondrites vary between those found in ordinary chondrites and those found in Earth[2–4].

We report high-precision Sm and Nd isotope measurements and Sm/Nd ratios of some of the earliest-formed objects in the Solar System. CAIs condensed from the solar nebula gas are the oldest dated materials in the Solar System[16]. The internal mineral isochron method has been applied to individual CAIs to determine the initial Solar System abundances of short-lived radionuclides for several radiogenic systems[17], including $^{146}Sm–^{142}Nd$ (ref. 18). In the Allende CV3 carbonaceous chondrite, CAIs can be affected by thermal metamorphism[18,19]. To avoid isotopic disturbances from metamorphism and to evaluate the extent of isotopic heterogeneities in CAIs, we selected inclusions that have previously been chemically and/or petrographically characterized and that have different crystallization histories (Methods). We investigated mineral separates (melilite and fassaite—a Ca, Al, Mg-rich silicate and an Al-rich pyroxene, respectively) and bulk sample powders of 1-cm-sized CAIs from the CV3-chondrite meteorites Northwest Africa (NWA) 2364 (the 'crucible', type B) and NWA 6991 (B4, compact type A; Extended Data Fig. 1) to constrain their internal Sm–Nd isotopic evolution. We also analysed as bulk powders two Allende fine-grained CAIs (Extended Data Fig. 1) that, on the basis of their fine-grained mineral textures, have not been melted since they condensed from the nebular gas. Primitive enstatite chondrites from petrologic type 3 of the EH (ALHA77295) and EL (MAC 02837 and MAC 02839) subgroups were also selected. The sulfide assemblages of these three enstatite chondrites indicate that they are the most pristine and unmetamorphosed enstatite chondrites available from the two subgroups[4,20], suggesting that they are the best candidates to preserve both their Sm and Nd elemental abundances and any isotopic heterogeneities inherited from their formation region in the solar nebula. For each sample, the abundances of Sm and Nd stable isotopes, including the minor proton-rich isotope ^{144}Sm (3.1% of total Sm), were measured with a precision of a few parts per million, along with the corresponding Sm/Nd elemental ratios (Supplementary Tables 1–3). Any modifications due to exposure to galactic cosmic rays were monitored, but this effect is small and does not induce any substantial modification of Nd isotope ratios (maximum 1 p.p.m.; Methods).

The two CAIs from NWA 2364 and NWA 6991 have $^{147}Sm–^{143}Nd$ ages in agreement with those obtained by U–Pb radiometric dating (ref. 16), showing that the Sm–Nd chronometers have not been disturbed by secondary processes (Extended Data Fig. 7a, b). Regression of $^{147}Sm/^{144}Nd–^{142}Nd/^{144}Nd$ (Fig. 1) for NWA 6991 fractions yields a $\mu^{142}Nd$ value of -8.4 ± 5.1 p.p.m. at a chondritic Sm/Nd ratio (mean square weighted deviation, MSWD = 0.76)—a value that is indistinguishable within errors from the terrestrial equivalent (0 ± 5 p.p.m.; 2 s.d., measured on JNdi-1 Nd isotopic standard). The NWA 2364 CAI regression is less well constrained (MSWD = 2.8), yielding a $\mu^{142}Nd$ value of -2.9 ± 25.4 p.p.m. (2 s.d.) at a chondritic Sm/Nd ratio. Therefore, internal isochron regression lines of two individual CAIs intersect the composition of the modern accessible Earth at a chondritic Sm/Nd ratio, which is the same as the Sm/Nd ratio of enstatite chondrites measured in this study (Fig. 1). These similar $\mu^{142}Nd$ values at chondritic Sm/Nd ratios for two CAIs are in contrast with the literature average values for enstatite, ordinary and carbonaceous chondrites, which are, in that order, increasingly deficient in ^{142}Nd (refs 2–4; Fig. 1). The CAIs have Sm isotope patterns with deficits in ^{144}Sm, ^{149}Sm and ^{154}Sm, and excesses in ^{148}Sm and ^{150}Sm (Fig. 2a). The large deficits in ^{144}Sm of up to -290 p.p.m. are clearly dominated by a proton-rich process (p-process) deficiency. The lack of correlation between ^{142}Nd and ^{144}Sm variations between Solar System objects characterized by different ^{144}Sm signatures indicates that the contribution of p-processes to ^{142}Nd is negligible, contrary to previous suggestions[4,21] (Extended Data Fig. 5). The positive $\mu^{148}Sm–\mu^{150}Sm$ correlation (Extended Data Fig. 3) shows that CAIs are the carrier of a slow-neutron-capture-process

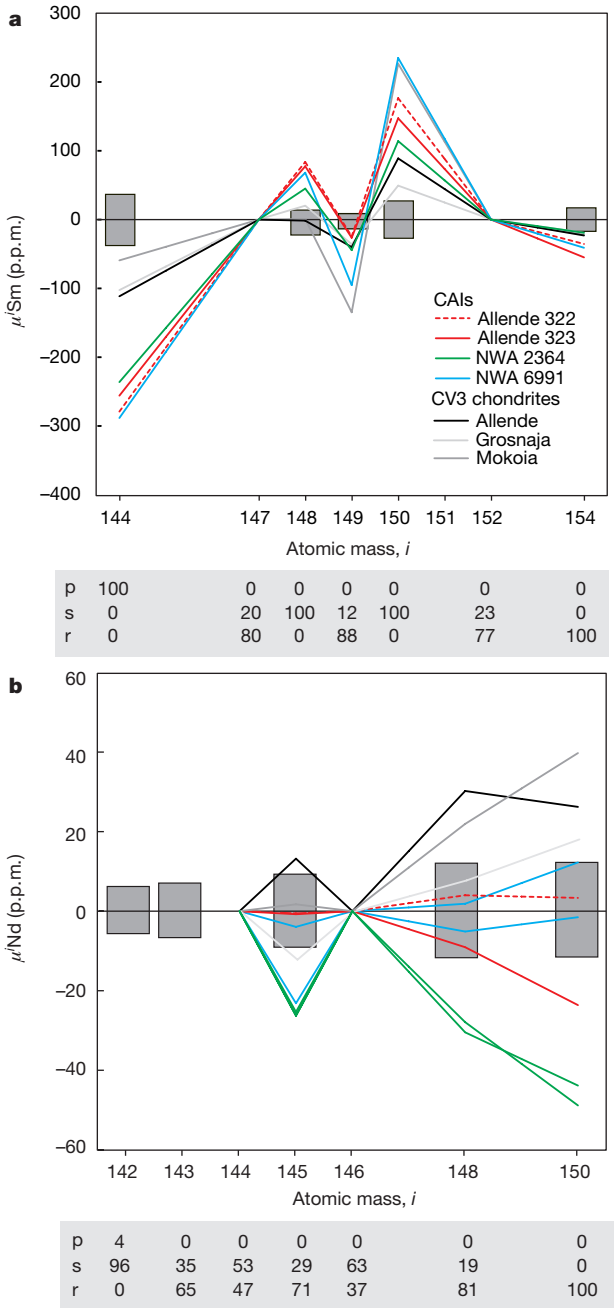

Figure 2 | Sm and Nd isotope compositions of bulk CAIs (leached and unleached) and CV3 whole-rocks. a, **b**, $\mu^i Sm$ (**a**) and $\mu^i Nd$ (**b**) represent the isotopic composition measured in meteorites relative to the isotope ratio measured in the terrestrial standard, and is given in parts per million. Sm and Nd data were corrected for instrumental mass fractionation using the exponential law and $^{147}Sm/^{152}Sm = 0.56081$ and $^{146}Nd/^{144}Nd = 0.7219$, respectively (Supplementary Tables 1–3). Grey boxes show the external reproducibility (2 s.d.) obtained on the standards. The relative contributions of the p-, s- and r-processes for stable and radiogenic (^{142}Nd and ^{143}Nd) isotopes are indicated (as percentages) below the plots[22]. The now-extinct ^{146}Sm is not represented, but is a pure p-process isotope. The two radiogenic Nd isotopes, ^{142}Nd and ^{143}Nd, are not represented because their deviations reflect mostly the radiogenic contribution.

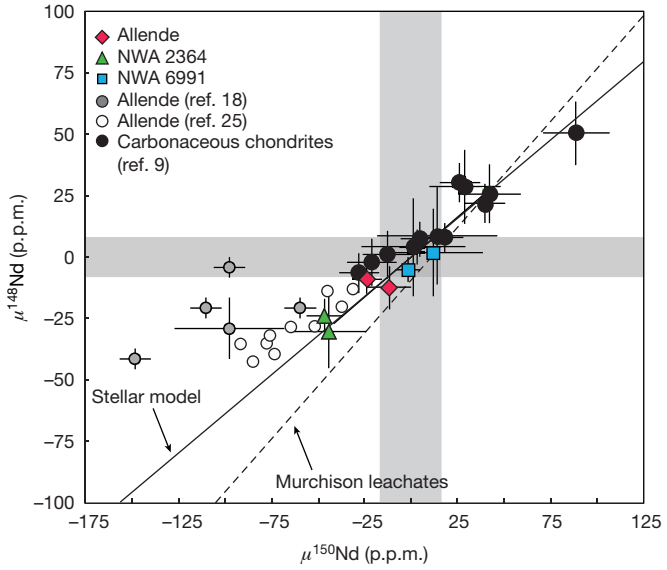

Figure 3 | ^{150}Nd/^{144}Nd versus ^{148}Nd/^{144}Nd measured in CAIs and carbonaceous chondrites. The data for carbonaceous chondrites are from ref. 9 and those for Allende CAIs are from refs 18 and 25. Error bars show the analytical uncertainty (2 s.e.); the grey boxes represent the external reproducibility (2 s.d.) obtained on the JNdi-1 standard. The internal errors for Allende bulk CAIs are not reported in ref. 25. The data plot on the mixing line calculated from isotope production in stellar models (solid black line)[22,26], but not on the regression defined by leachate Nd isotopic data of the CM2 chondrite Murchison (dashed black line)[24]. The signatures in ^{148}Nd and ^{150}Nd of the Allende 322 and 323 and NWA 6991 CAIs are not different from the terrestrial standard considering the analytical uncertainties.

(s-process) excess and a rapid-neutron-capture-process (r-process) deficit in CV chondrites. The stable Nd isotope compositions of the bulk CAIs and their mineral fractions are similar to the terrestrial values within analytical error, except for the NWA 2364 CAI, which has deficits in ^{145}Nd, ^{148}Nd and ^{150}Nd (Fig. 2b). We identified a CAI in CV3 NWA 6991 that is petrogenetically primitive (Methods) and shares an identical Nd stable isotopic composition with Earth. Because different mineral fractions have been separated, the radiogenic ^{142}Nd isotope of NWA 6991 can be compared to the value for Earth without the need for any correction for neutron capture or nucleosynthetic anomalies. Its μ^{142}Nd value at a chondritic Sm/Nd ratio is -8.4 ± 5.1 p.p.m., which is indistinguishable within errors from the terrestrial value (0 ± 5 p.p.m.). By contrast, the s-process excesses and r-process deficits identified in the Nd stable isotopes of NWA 2364 CAIs should substantially increase the ^{142}Nd/^{144}Nd ratios (Fig. 2a, b). The correction for ^{142}Nd is complex and its accuracy is difficult to evaluate. Isotopes from the same element should be used to correct for nucleosynthetic effects[3]. A correction of -25 p.p.m. on ^{142}Nd is calculated using different approaches: (i) by using the ^{142}Nd–^{148}Nd relationship calculated from a stellar model ($\mu^{148}\text{Nd} = -1.01 \times \mu^{142}\text{Nd}$; ref. 22); (ii) by using the isotope composition measured in SiC as representative of a pure s-process component ($\mu^{148}\text{Nd} = -1.15 \times \mu^{142}\text{Nd}$; ref. 23); and (iii) by considering the correlation in leachates data obtained on carbonaceous chondrites ($\mu^{148}\text{Nd} = -0.96 \times \mu^{142}\text{Nd}$; ref. 24). A smaller correction of 14 p.p.m. to the ^{142}Nd/^{144}Nd ratio was calculated for the Allende Al3S4 CAI[18], whereas the separated mineral fractions of Al3S4 were characterized by the highest deficits in both ^{148}Nd and ^{150}Nd measured in CAIs. We note that the mineral separates from Allende Al3S4 CAI have different μ^{148}Nd and μ^{150}Nd values[18] that do not fall on the correction line between CAIs and carbonaceous chondrites (Fig. 3). In contrast, carbonaceous chondrites and bulk CAIs from this study and from ref. 25 plot on the μ^{148}Nd–μ^{150}Nd mixing line calculated from isotope production in stellar models[22,26] represented in Fig. 3. These CAIs do not fall on the regression line defined by Nd isotopic data of leachates of the CM2 chondrite Murchison[24], which instead plot towards the composition of presolar SiC grains. Ultimately, after correcting for nucleosynthetic anomalies and radiogenic decay, CAIs show a range of ^{142}Nd/^{144}Nd ratios similar to enstatite chondrites, with values between the modern terrestrial average composition and those of ordinary chondrites. Furthermore, our data on enstatite chondrites have a range of ^{147}Sm/^{144}Nd ratios from 0.1948 to 0.1958, within 1% of the chondritic uniform reservoir (CHUR) value of 0.1960 (ref. 27), and do not show any correlation between μ^{142}Nd and μ^{144}Sm anomalies, in contrast to a previous study (Extended Data Fig. 5). We can therefore calculate the initial and modern compositions at a common chondritic ^{147}Sm/^{144}Nd without any model dependence and without introducing large errors on initial ^{142}Nd abundance. We calculate μ^{142}Nd values from -3 p.p.m. to -9 p.p.m. when normalized at the CHUR ^{147}Sm/^{144}Nd ratio (Supplementary Table 1). From our data, we obtain an average enstatite chondrite composition with $\mu^{142}\text{Nd} = -7 \pm 6$ p.p.m. (2. s.d.; $n = 3$), which is indistinguishable within errors from the composition of Earth's mantle of 0 ± 5 p.p.m. (Fig. 1). The dataset presented in ref. 4 had more scattered Sm/Nd ratios, which introduced uncertainties when correcting for ^{142}Nd produced by radiogenic decay and when normalizing ^{142}Nd/^{144}Nd ratios of individual whole-rock chondrites to a common CHUR Sm/Nd ratio. Nevertheless, we calculate a combined average for EL and EH chondrites (data from this study and ref. 4) of $\mu^{142}\text{Nd} = -9 \pm 17$ p.p.m. (2 s.d.; $n = 13$ individual enstatite chondrites), which is less precise, but remains consistent with Earth's composition.

We find that several early Solar System objects, including CAIs and enstatite chondrites, share a common Nd stable isotope signature with modern terrestrial samples, even though these materials sample spatially or temporally distinct regions of the protoplanetary disk. The CAIs formed under reduced conditions, closest to the proto-star, before being transported outward to the accretion regions of the chondrite groups[28]. The reduced enstatite chondrites are suggested to have formed within the inner fringe of the asteroid belt, and the more oxidized ordinary chondrites and carbonaceous chondrites in the outer parts[29]. Our results therefore suggest a relationship between ^{142}Nd abundance and heliocentric distance. Materials formed in the inner region of the Solar System have the highest ^{146}Sm decay-normalized ^{142}Nd/^{144}Nd ratios, followed by whole-rock ordinary chondrites and carbonaceous chondrites. The amount of material required to have been hidden within or lost from Earth was previously constrained using ^{142}Nd abundances measured in ordinary chondrites (see, for example, refs 5, 9). Although the building blocks of Earth are difficult to identify on the basis of meteorites that escaped accretion, enstatite chondrites are closest to Earth's composition when looking at the abundance of ^{142}Nd and of many other refractory elements[14]. Using the enstatite chondrite group as an isotope analogue of the accreting material that formed Earth, the calculated ^{147}Sm/^{144}Nd ratio of the silicate Earth would be 0.200, which is 2% higher than the CHUR ^{147}Sm/^{144}Nd ratio and within the range of values previously measured for whole-rock chondrites[27]. An external constraint on the Sm/Nd ratio for Earth arises from the combined Sm–Nd and Lu–Hf systematics of lunar samples, suggesting a chondritic Sm/Nd evolution of the bulk Moon[30]. Therefore, our results on CAIs together with those obtained on enstatite chondrites and lunar samples indicate that the Earth–Moon system evolved from a common isotopic reservoir in ^{142}Nd, with Sm/Nd proportions within 2% of the average of unequilibrated whole-rock chondrites[27]. The increasing number of measurements of the ^{146}Sm–^{142}Nd systematics of Solar System objects calls into question the notion of a super-chondritic Earth for refractory elements. Instead, our results indicate that variations in ^{142}Nd abundances found in planetary materials compared to the modern Earth are caused by nucleosynthetic anomalies, and eliminate the need for untapped or missing planetary reservoirs to explain the ^{146}Sm–^{142}Nd isotope systematics of terrestrial rocks[5,6].

Online Content Methods, along with any additional Extended Data display items and Source Data, are available in the online version of the paper; references unique to these sections appear only in the online paper.

Received 20 December 2015; accepted 4 August 2016.

1. Nyquist, L. E. *et al.* ^{146}Sm-^{142}Nd formation interval for the lunar mantle material. *Geochim. Cosmochim. Acta* **59,** 2817–2837 (1995).
2. Boyet, M. & Carlson, R. W. ^{142}Nd evidence for early (>4.53 Ga) global differentiation of the silicate Earth. *Science* **309,** 576–581 (2005).
3. Carlson, R. W., Boyet, M. & Horan, M. Chondrite barium, neodymium, and samarium isotopic heterogeneity and early Earth differentiation. *Science* **316,** 1175–1178 (2007).
4. Gannoun, A., Boyet, M., Rizo, H. & El Goresy, A. ^{146}Sm–^{142}Nd systematics measured in enstatite chondrites reveals a heterogeneous distribution of ^{142}Nd in the solar nebula. *Proc. Natl Acad. Sci.* **108,** 7693–7697 (2011).
5. Jellinek, A. M. & Jackson, M. G. Connections between the bulk composition, geodynamics and habitability of Earth. *Nat. Geosci.* **8,** 587–593 (2015).
6. O'Neill, H. S. C. & Palme, H. Collisional erosion and the non-chondritic composition of terrestrial planets. *Philos. Trans. R. Soc. Lond. A* **366,** 4205–4238 (2008).
7. Kinoshita, N. *et al.* A shorter ^{146}Sm half-life measured and implications for ^{146}Sm-^{142}Nd chronology in the Solar System. *Science* **335,** 1614–1617 (2012).
8. Boyet, M., Carlson, R. W. & Horan, M. Old Sm-Nd ages for cumulate eucrites and redetermination of the Solar System initial ^{146}Sm/^{144}Sm ratio. *Earth Planet. Sci. Lett.* **291,** 172–181 (2010).
9. Caro, G., Bourdon, B., Halliday, A. N. & Quitté, G. Super-chondritic Sm/Nd ratios in Mars, the Earth and the Moon. *Nature* **452,** 336–339 (2008).
10. Clayton, R. N., Hinton, R. W. & Davis, A. M. Isotopic variations in the rock-forming elements in meteorites. *Philos. Trans. R. Soc. Lond. A* **325,** 483–501 (1988).
11. Anders, E. & Zinner, E. K. Interstellar grains in primitive meteorites: diamond, silicon carbide, and graphite. *Meteoritics* **28,** 490–514 (1993).
12. Trinquier, A. *et al.* Origin of nucleosynthetic isotope heterogeneity in the solar protoplanetary disk. *Science* **324,** 374–376 (2009).
13. Moynier, F. *et al.* Planetary-scale strontium isotopic heterogeneity and the age of volatile depletion of early Solar System materials. *Astrophys. J.* **758,** 45 (2012).
14. Warren, P. H. Stable-isotopic anomalies and the accretionary assemblage of the Earth and Mars: a subordinate role for carbonaceous chondrites. *Earth Planet. Sci. Lett.* **311,** 93–100 (2011).
15. Clayton, R. N., Mayeda, T. K. & Rubin, A. E. Oxygen isotopic compositions of enstatite chondrites and aubrites. *Lunar Planet. Sci. Conf. Proc.* **15,** C245–C249 (1984).
16. Bouvier, A. & Wadhwa, M. The age of the Solar System redefined by the oldest Pb–Pb age of a meteoritic inclusion. *Nat. Geosci.* **3,** 637–641 (2010).
17. Kita, N. T. *et al.* ^{26}Al-^{26}Mg isotope systematics of the first solids in the early Solar System. *Meteorit. Planet. Sci.* **48,** 1383–1400 (2013).
18. Marks, N. E. *et al.* Samarium–neodymium chronology and rubidium–strontium systematics of an Allende calcium–aluminum-rich inclusion with implications for ^{146}Sm half-life. *Earth Planet. Sci. Lett.* **405,** 15–24 (2014).
19. Meeker, G. P., Wasserburg, G. J. & Armstrong, J. T. Replacement textures in CAI and implications regarding planetary metamorphism. *Geochim. Cosmochim. Acta* **47,** 707–721 (1983).
20. Gannoun, A., Boyet, M., El Goresy, A. & Devouard, B. REE and actinide microdistribution in Sahara 97072 and ALHA77295 EH3 chondrites: a combined cosmochemical and petrologic investigation. *Geochim. Cosmochim. Acta* **75,** 3269–3289 (2011).
21. Andreasen, R. & Sharma, M. Solar nebula heterogeneity in p-process samarium and neodymium isotopes. *Science* **314,** 806–809 (2006).
22. Arlandini, C. *et al.* Neutron capture in low-mass asymptotic giant branch stars: cross sections and abundance signatures. *Astrophys. J.* **525,** 886–900 (1999).
23. Hoppe, P. & Ott, U. Mainstream silicon carbide grains from meteorites. *AIP Conf. Proc.* **402,** 27–58 (1997).
24. Qin, L., Carlson, R. W. & Alexander, C. M. O. D. Correlated nucleosynthetic isotopic variability in Cr, Sr, Ba, Sm, Nd and Hf in Murchison and QUE 97008. *Geochim. Cosmochim. Acta* **75,** 7806–7828 (2011).
25. Brennecka, G. A., Borg, L. E. & Wadhwa, M. Evidence for supernova injection into the solar nebula and the decoupling of r-process nucleosynthesis. *Proc. Natl Acad. Sci. USA* **110,** 17241–17246 (2013).
26. Bisterzo, S. *et al.* Galactic chemical evolution and solar s-process abundances: dependence on the ^{13}C-pocket structure. *Astrophys. J.* **787,** 10 (2014).
27. Bouvier, A., Vervoort, J. D. & Patchett, P. J. The Lu-Hf and Sm-Nd isotopic composition of CHUR: constraints from unequilibrated chondrites and implications for the bulk composition of terrestrial planets. *Earth Planet. Sci. Lett.* **273,** 48–57 (2008).
28. Simon, J. I. *et al.* A short timescale for changing oxygen fugacity in the solar nebula revealed by high-resolution ^{26}Al–^{26}Mg dating of CAI rims. *Earth Planet. Sci. Lett.* **238,** 272–283 (2005).
29. Jacquet, E. Transport of solids in protoplanetary disks: comparing meteorites and astrophysical models. *C. R. Geosci.* **346,** 3–12 (2014).
30. Sprung, P., Kleine, T. & Scherer, E. E. Isotopic evidence for chondritic Lu/Hf and Sm/Nd of the Moon. *Earth Planet. Sci. Lett.* **380,** 77–87 (2013).

Supplementary Information is available in the online version of the paper.

Acknowledgements Meteorite samples were provided by L. Garvie (Arizona State University), D. Ebel (American Museum of Natural History) and the US Antarctic Search for Meteorites (ANSMET) programme, which has been funded by NSF and NASA, and were characterized and curated by the Department of Mineral Sciences of the Smithsonian Institution and Astromaterials Curation Office at NASA Johnson Space Center. We thank P. J. Patchett for the Sm–Nd calibrated enriched spike used in this study, D. Auclair and A. Gannoun for mass spectrometer support, and T. Withers for comments on this Letter. This research was supported by the National Science Foundation NSF/EAR 1119135, France-Canada Research Fund, NSERC Canada Research Chair and Discovery Grant awards to A.B. and the French Government ANR-10-LABX-0006, the Région Auvergne, the European Regional Development Fund and the INSU Programme National de Planétologie to M.B. We thank the Laboratory of Excellence ClerVolc.

Author Contributions A.B. and M.B. planned and carried out the analyses for the project and wrote the manuscript.

Author Information Reprints and permissions information is available at www.nature.com/reprints. The authors declare no competing financial interests. Readers are welcome to comment on the online version of the paper. Correspondence and requests for materials should be addressed to A.B. (audrey.bouvier@uwo.ca).

METHODS

Samples and analytical methods. Calcium–aluminium-rich inclusions (CAIs) were obtained from the Center for Meteorite Studies at Arizona State University for Allende (named 322 and 323) and Northwest Africa (NWA) 6991 (named B4, fragment mass of about 150 mg), and from the American Museum of Natural History in New York for NWA 2364 (named the 'crucible', fragment mass of about 150 mg). For Allende, the two small (50–100 mg), fine-grained (unmelted) CAIs were processed as bulk powders. These four CAIs were selected on the basis of their petrogenetic differences, to assess potential Sm and Nd stable isotopic heterogeneities linked to different CAI groups and formation histories. Geochemical studies of fine-grained CAIs in CV3 chondrites indicate that they did not melt and that they belong to group II CAIs, on the basis of their rare-earth elemental abundances[31]. These characteristics point towards formation as a gas–solid condensate from the nebular gas with minor reprocessing[31]. The Sm and Nd concentrations normalized to CI chondrites are $Sm_N = 19–20$ and $Nd_N = 20–22$. The lower, normalized Lu concentrations of $Lu_N = 0.3–3$ (concentrations in Extended Data Table 1) that were measured in these two CAIs by isotopic dilution point towards a fractionated rare-earth element (REE) pattern and a group II classification for both Allende CAIs 322 and 323 (Extended Data Fig. 1). The inclusion B4 of NWA 6991 was petrographically characterized[2] as a compact type A CAI. The CAIs B4 and crucible were processed for mineral separation. Mineral separates (melilite and fassaite) were concentrated from a 30–63-μm fraction using bromoform and methylene iodide heavy liquids, and hand picking as described in ref. 16. The same CAI B4 has been dated using the Al–Mg and U–Pb radiogenic decay systems at 4,567.94 ± 0.31 Myr (ref. 32). Bulk samples were processed at Arizona State University (Allende) and the University of Minnesota (NWA 6991 and NWA 2364) as unleached and as leached with 10% HF and, subsequently, with 20% HCl for 20 min each at room temperature. Mineral separates were similarly leached before dissolution. The leachates were not analysed for ^{146}Sm–^{142}Nd systematics owing to the limited leached sample masses.

Enstatite chondrites were obtained from the US Antarctic meteorite collection. Chips of about 1.2–1.4 g of enstatite chondrites MacAlpine Hills (MAC) 02837, 26, MAC 02839, 12 and Allan Hills A77295 (ALHA77295 or ALH 77295), 74 were crushed in an agate mortar and pestle into fine whole-rock powders by separating and remixing the metal to preserve all components together before acid digestion.

New PFA Savillex beakers were used for these samples to avoid memory effects. Parr bombs with 14-ml insert PTFE vials were not previously exposed to enriched spikes and were used for only meteorite dissolution. Only MilliQ Millipore water, BDH Aristar Ultra hydrofluoric and hydrochloric acids, and triple sub-boiled quartz-distilled nitric acid were used for all steps.

For enstatite chondrites, the whole-rock powders were dissolved using a first step in concentrated HF-HNO_3 (10:1) at 120 °C on a hot plate for 2 days to liberate hydrogen sulfide and silicate tetrafluoride gases before transferring the residues into Parr pressured vials. For CAIs and enstatite chondrites, samples were placed into individual Parr bomb pressured vials in concentrated HF-HNO_3 (10:1) for 7 days at 155 °C. After drying down the samples, perchloric acid was added and evaporated at 200 °C on a hot plate to break down the fluorides, and samples were taken back into solution in Parr bomb pressured vials in 6 M HCl for 2 days at 155 °C. Solutions were transferred into Savillex PFA beakers and split into an approximately 90% fraction for isotopic composition, an approximately 5%–10% fraction spiked with an enriched ^{149}Sm–^{150}Nd mixed spike for isotopic dilution to determine the Sm/Nd ratio (using the measured stable Sm and Nd isotopic compositions), and an approximately 5% fraction for inductively coupled plasma mass spectrometry (ICPMS) analysis for trace element abundances for the NWA 6991 CAI bulk sample (Extended Data Fig. 1). The CAI B4 has a flat REE pattern normalized to CI chondrites ((17–20) × CI chondrites) with slight positive Eu anomaly ($Eu_N = 23$) corresponding to a chemical group I CAI[7]. The same group I is suggested for NWA 2364 unleached bulk CAI with $Sm_N = 17$, $Nd_N = 16$ and $Lu_N = 20$ (CI-chondrite normalized REE concentrations shown in Extended Data Fig. 1 and concentrations given in Extended Data Table 1).

All Sm and Nd concentrations obtained by isotope dilution are reported in Extended Data Table 1. Sm and Nd in the spiked fractions were purified and separated using a two-stage chemistry procedure. The REEs were first separated from the matrix using a 2-ml or 8-ml cation resin AG50W-X8 column. The REE fraction was then loaded in 0.14 M HCl onto a 1-ml Eichrom Ln-spec resin bed to separate the Nd and Sm fractions in 0.14 M HCl and 0.40 M HCl, respectively. The chemistry procedure was different for the unspiked fractions. After the first 8-ml cation columns, the REE fractions were processed twice through a cation column using 2-methylactic acid (0.2 M, pH 4.7) with a small amount of H_2O_2. The Sm fraction was collected before the Nd fraction during the first chemistry, but at this stage heavier REEs were still present within the two collected fractions. The last step consists of one pass through Ln-spec resin in weak HCl. This procedure ensures perfect separation of Nd from Ce and Sm by reducing the effect of interferences on mass 142 from Ce and on masses 144, 148 and 150 from Sm, and the purification of the Sm fraction (Gd interferes at masses 152 and 154). Organic residues are then completely removed using hydrogen peroxide and the sample is ready to be loaded on a Re filament. Total procedural blanks for Sm and Nd were 3 pg and 10 pg, respectively. The blank contribution to each sample was negligible, with Sm and Nd fractions of at least 80 ng for the smallest analysed sample.

Spiked Sm and Nd isotopic fractions for the isotopic dilution method were analysed in static mode using a MC-ICPMS Neptune at Arizona State University for Allende CAIs, and Neptune Plus at the University of Minnesota and the Laboratoire Magmas et Volcans (Clermont-Ferrand, France) for the NWA 6991 and NWA 2364 CAIs using methods described in ref. 27. AMES Sm and JNdi-1 Nd standards were used to control mass bias and cup efficiency during all the sessions. The calculated Sm and Nd concentrations and $^{147}Sm/^{144}Nd$ ratio of samples are reported in Supplementary Table 1. Additionally, a BCR-2 rock standard was processed and analysed in each laboratory, and Sm and Nd concentrations and calculated $^{147}Sm/^{144}Nd$ and $^{143}Nd/^{144}Nd$ ratios are reported in Supplementary Table 1.

Sm and Nd isotopes of unspiked fractions were obtained on the ThermoFisher Triton thermal ionization mass spectrometer at the Laboratoire Magmas et Volcans. The purified Sm and Nd cuts were loaded in 2.5 M HCl on outgassed, zone-refined Re filaments. The Sm was measured in static mode as Sm^+. The Faraday cup configuration was centred at mass 149 and Nd and Gd interferences were monitored at masses 146 (cup L3) and 156 (cup H4). Each run consisted of 18 to 27 blocks of 20 cycles using amplifier rotation with background acquisition before each block. Sample measurements were in general shorter depending on the amount loaded (see Supplementary Table 2). Signals for ^{152}Sm ranged between 0.5×10^{-11} A and 3.5×10^{-11} A for standards and between 0.5×10^{-11} A and 2.0×10^{-11} A for samples. Sm data were corrected for instrumental mass fractionation using the exponential law and $^{147}Sm/^{152}Sm = 0.56081$. Sm isotope compositions for standards and samples are given in Supplementary Table 2. Sm isotope compositions were measured during three different periods, called session #1 to #3 in Supplementary Table 2. The μ values correspond to deviations relative to the standard value, expressed in parts per million. In static mode, the ratios evolve with time owing to cup ageing. Consequently, we used the average of ratios measured on standards during the same analytical session for calculating the sample μ values. The external reproducibility calculated from repeated measurements of the standard (5–7 standards measured per analytical session) is 15–37 p.p.m. on $^{144}Sm/^{152}Sm$, 5–18 p.p.m. on $^{148}Sm/^{152}Sm$, 7–11 p.p.m. on $^{149}Sm/^{152}Sm$, 14–27 p.p.m. on $^{150}Sm/^{152}Sm$ and 12–17 p.p.m. on $^{154}Sm/^{152}Sm$. The Nd samples were measured as Nd^+ using 9 Faraday cups. We used a dynamic procedure (axial cup centred at masses 143 and 145) to measure the $^{142}Nd/^{144}Nd$ ratios in dynamic mode; all other ratios were measured in static mode (line 1 centred at 145). Ce and Sm interferences on masses 142 and 144 were monitored using masses 140 and 147, respectively. Ce and Sm contributions on masses 142 and 144 were lower than 3 p.p.m. for standard and sample measurements, except for sample NWA 6991, in which the Sm contribution on mass 144 reaches 15 p.p.m. Nd isotope ratios were corrected for mass fractionation to $^{146}Nd/^{144}Nd = 0.7219$ using the exponential law. The external reproducibility (2 s.d.) calculated from repeated measurements of the standard within each session is 4–6 p.p.m. on $^{142}Nd/^{144}Nd$, 3–7 p.p.m. on $^{143}Nd/^{144}Nd$, 4–8 p.p.m. on $^{145}Nd/^{144}Nd$, 3–12 p.p.m. on $^{148}Nd/^{144}Nd$ and 10–12 p.p.m. on $^{150}Nd/^{144}Nd$ (Supplementary Table 3).

Sm isotopes. The Sm isotopic compositions measured for terrestrial standards and samples are presented in Supplementary Table 2. For samples measured during the first sequence, the quantity of Nd is substantially higher than that present in the Sm standard. Nevertheless, there is no correlation between Sm isotope ratios and the quantity of Nd found in our samples (Extended Data Fig. 2). The ^{144}Sm deficits in all bulk CAI samples are in the range −236 p.p.m. to −288 p.p.m. and do not correlate with Nd/Sm (Extended Data Fig. 2). The melilite fraction of the NWA 2364 CAI has the lowest deficit in ^{144}Sm ($\mu^{144}Sm = -113$ p.p.m.) and lower Sm isotope anomalies than other CAI fractions in general. This sample was measured with the lowest Sm intensity and during a very short period (60 ratios), so isotopic ratios have a precision that is three times lower than those of the other samples. All CAI fractions, except for the NWA 6991 leached bulk fraction and the melilite from NWA 2364, have excesses in ^{148}Sm (+45 p.p.m. to +84 p.p.m.), deficits in ^{149}Sm (−25 p.p.m. to −95 p.p.m.), excesses in ^{150}Sm (+114 p.p.m. to +240 p.p.m.) and deficits in ^{154}Sm (−18 p.p.m. to −54 p.p.m.). The Sm isotope patterns are presented in Fig. 2a. In this representation, the Sm isotopes at masses 147 and 152 are equal to zero because measured data are normalized using the $^{147}Sm/^{152}Sm$ ratio.

Deficits in ^{144}Sm can reflect deficits in p-process isotopes, but they are also artificially created by s-process excess and/or r-process deficits using the $^{147}Sm/^{152}Sm$ normalization scheme. The two Sm isotopes used for mass bias correction are predominantly formed by r-processes (88% and 77% for ^{147}Sm and ^{152}Sm, respectively), and the remaining part is formed by s-processes. The positive

μ^{148}Sm–μ^{150}Sm correlation (Extended Data Fig. 3) shows that CAIs are the carrier of an s-process excess and an r-process deficit. This correlation is in agreement with the general shape of the pattern, with deficits in ^{144}Sm, ^{149}Sm and ^{154}Sm, and excesses in ^{148}Sm and ^{150}Sm (Fig. 2a). The NWA 6991 CAI has the highest deficits in ^{149}Sm and highest excesses in ^{150}Sm, and this sample does not fall on the μ^{148}Sm–μ^{150}Sm correlation line formed by CV3 chondrites and other CAIs[25]. This result suggests that the Sm isotope composition of the NWA 6991 CAI has been modified by neutron fluence capture, owing to long-term exposure to galactic cosmic rays following the reaction ^{149}Sm(n, γ)^{150}Sm. Nevertheless, this effect is small and does not induce any substantial modification of Nd isotope ratios because Nd isotopes have smaller neutron capture cross sections than does ^{149}Sm (ref. 1). CAIs and carbonaceous chondrites plot on the same correlation line, which intersects the ^{148}Sm terrestrial value at μ^{144}Sm = −60 p.p.m. in the μ^{144}Sm–μ^{148}Sm diagram (Extended Data Fig. 3). This value is in agreement with the deficit in ^{144}Sm of about −80 p.p.m. measured in carbonaceous chondrites that have terrestrial ^{148}Sm abundances[3,21]. The CAIs represent the end-member farthest from the terrestrial composition. The three enstatite chondrites have terrestrial compositions for both ^{148}Sm and ^{154}Sm, indicating that the ^{149}Sm–^{150}Sm signature (excess in ^{149}Sm coupled to deficit in ^{150}Sm) reflects secondary reactions. Deficit or excess in s-processes must generate similar deviations in both ^{148}Sm/^{152}Sm and ^{150}Sm/^{152}Sm ratios. The two EL3 samples MAC 02837 and 02839 have variable ^{144}Sm abundances with μ values of −3 ± 16 p.p.m. and 48 ± 12 p.p.m., respectively.

Nd isotopes. The Nd isotopic compositions measured for CAIs and enstatite chondrite samples are presented in Supplementary Table 3. ^{142}Nd/^{144}Nd ratios were measured in static and dynamic modes. Data are compared in Extended Data Fig. 4 and ratios fall on the 1:1 line. The contribution of Ce and Sm measured in JNdi-1 standard and samples is negligible, with the exception of the NWA 2364 CAI measured during the third session, in which the cerium correction on the ^{142}Nd/^{144}Nd ratio is 560 p.p.m. The stable Nd isotope compositions of the bulk CAIs and their mineral fractions are similar to the terrestrial values within the analytical error, except for the NWA 2364 CAI, which has deficits in ^{145}Nd (μ = −26 ± 4 p.p.m.), ^{148}Nd (μ = −25 ± 6 p.p.m.) and ^{150}Nd (μ = −48 ± 9 p.p.m.) (Fig. 2b). As observed for Sm isotopes, this signature results from s-process excesses and r-process deficits. The Nd isotope patterns are presented in Fig. 2b. Using this representation, the Nd at masses 144 and 146 are equal to zero, because the measured data are normalized using the ^{146}Nd/^{144}Nd ratio. For Nd isotopes in enstatite chondrites, MAC 02837 has a terrestrial abundance in ^{142}Nd (μ = −6 ± 7), whereas MAC 02839 and ALHA77295 have small deficits (μ = −10 ± 6 and μ = −11 ± 3, respectively). For stable isotopes, the abundances are identical to those measured in Nd standards and terrestrial samples, except for MAC 02837, which has a deficit of −115 ± 9 p.p.m. in ^{150}Nd abundance. Because all other Nd isotopes are present in terrestrial abundances, the cause of this deficit in ^{150}Nd is unclear.

Neutron fluence effect on the Sm isotope patterns of CAIs. The Sm isotope patterns for CAIs have deficits in ^{149}Sm and excesses in ^{150}Sm. The negative correlation between the ^{149}Sm/^{152}Sm and ^{150}Sm/^{152}Sm ratios (Extended Data Fig. 3) may reflect deficits or excesses in s- and r- process nuclides because ^{149}Sm is dominated by r-processes (88%), whereas ^{150}Sm is a pure s-process nuclide. This correlation can also be created by nuclear reactions induced by interaction between galactic cosmic rays and the surface of extraterrestrial material. At low energy, epithermal and thermal neutron reactions produce nuclides by neutron capture. ^{149}Sm has the largest neutron capture cross-section of all Sm isotopes and the reaction ^{149}Sm(n, γ)^{150}Sm is commonly used for estimating the amplitude of this secondary nuclear reaction in lunar samples (black line in Extended Data Fig. 3a drawn from lunar data[33]). Nuclear reactions induced by exposure to galactic cosmic rays are the result of a surface process that becomes negligible at relatively small depths (below 2–3 m; ref. 34). The deficits in ^{149}Sm measured in Allende CAIs (−25 p.p.m. to −31 p.p.m.) are similar to those measured in the different dissolutions of the Allende bulk sample[3,21], but the excesses in ^{150}Sm in CAIs (+147 p.p.m. to +176 p.p.m.) are higher than those measured in the whole rocks (+90 p.p.m.). The Sm isotope patterns of Allende CAIs are not affected by neutron fluence. The NWA 6991 CAI has both a higher deficit in ^{149}Sm (−95 p.p.m.) and a higher excess in ^{150}Sm (+235 p.p.m.) than other CAIs measured in this study, and plots close to the whole-rock CV3 Mokoia in Fig. 2a (data from ref. 3). The NWA 6991 CAI also falls far from the regression line for Allende, NWA 2364 and the CV3 whole-rock chondrites in the μ^{148}Sm–μ^{150}Sm diagram (except Mokoia, Extended Data Fig. 3b). Because ^{148}Sm and ^{150}Sm are pure s-process nuclides, the two ^{148}Sm/^{152}Sm and ^{150}Sm/^{152}Sm ratios should be positively correlated for samples that have not been affected by interaction with galactic cosmic rays. The excess observed in ^{150}Sm for the NWA 6991 CAI is explained by secondary production of this isotope, and, using the correlation plotted in Extended Data Fig. 3b, we can estimate an increase in μ^{150}Sm of about 100 p.p.m. Using the ^{149}Sm–^{150}Sm relationships established for lunar samples[33], we calculate that an excess of about 100 p.p.m. in ^{150}Sm should correspond to a decrease in μ^{149}Sm of about 40 p.p.m. Such a variation will have a negligible effect (<1 p.p.m.) on the corrected ^{142}Nd/^{144}Nd ratio, considering the relationship[1,35] between Sm and Nd isotopes.

P-process contribution to ^{142}Nd production. ^{142}Nd is not a pure s-process isotope, but contains a small fraction of p-process isotope that varies between 4% and 20%, with the lower estimate obtained from stellar nucleosynthesis models[36] and the upper estimate from measurements of meteorites[4]. By monitoring the abundance of the pure p-process ^{144}Sm isotope in CAIs, we evaluate how this process affects the corresponding ^{142}Nd/^{144}Nd ratio. The Sm isotope patterns of all CAIs are similar to those measured in CV3 chondrites, but the anomalies (whether excess or deficit) are commonly larger (Fig. 2a), with two major differences. First, CAIs have large deficits in ^{144}Sm, up to −290 p.p.m. relative to the bulk CV (−100 p.p.m. on average[3,21]). Second, they have small excesses in ^{148}Sm, whereas CV3 chondrites have terrestrial ^{148}Sm abundances. Deficits in ^{144}Sm can reflect deficits in p-process isotopes, but apparent deficits may also arise from the ^{147}Sm/^{152}Sm normalization used to correct instrumental mass bias when applied to samples with s-process excesses and/or r-process deficits. The contribution of the deficits induced by the normalization is estimated using stellar models[22,26], and shows that the ^{144}Sm deficit should be about 25% of the excess in ^{148}Sm, which corresponds to a maximum deficit of 15 p.p.m. in ^{144}Sm. The measured deficits in μ^{144}Sm of >200 p.p.m. in CAIs are therefore clearly dominated by a p-process deficit.

It has been shown[36] that a fractionated Nd/Sm p-process isotope contribution ratio resulting from chemical separation upon condensation in a circumstellar environment could also explain the μ^{144}Sm–μ^{142}Nd isotope correlation found in ref. 4, with as little as 4% p-process contribution on ^{142}Nd. Combined Sm–Nd isotope measurements of different Solar System objects show that materials with a large range of μ^{144}Sm values have identical μ^{142}Nd compositions, as illustrated for the measured CAIs and the FUN (fractionated and unknown nuclear effects) inclusion C1 in Extended Data Fig. 5. The CAIs and FUN C1 fall on the 1% p-process–99% s-process ^{142}Nd line, which suggests that the contribution of p-process to ^{142}Nd is negligible and within our measurement errors. Moreover, after including our enstatite chondrite data, the μ^{144}Sm–μ^{142}Nd correlation that had been previously found between the different groups of chondrites[4] is no longer present. Only the carbonaceous chondrites are clearly distinct, with the highest deficits in both ^{144}Sm and ^{142}Nd. All the different mineral fractions and the bulk CAIs show excesses in s-process isotopes and deficits in r-process isotopes for Sm, whereas deviations in Nd isotope ratios relative to the terrestrial standard are observed for only NWA 2364 (Fig. 2b). Our data also confirm the variations in r-process deficits with a stronger effect on Sm in comparison to Nd (ref. 25).

The abundance of p-process isotopes relative to mass is shown in Extended Data Fig. 6. For isotopes formed by both p- and s-processes, the contribution of p-process isotopes are calculated using data from ref. 22 as the solar abundance minus the contribution of the s-process isotopes. The abundance of p-processes (normalized to Si) was recalculated using the total abundance of isotopes given in ref. 37. Extended Data Fig. 6 shows that the relation is well approximated by a power law. The abundance of pure p-process nuclides falls close to the curve. However, when we compare abundances calculated for 'mixed' isotopes (formed by mixing of p- and s-process isotopes such as ^{76}Se, ^{80}Kr, ^{142}Nd, ^{152}Gd and ^{164}Er), the abundances fall far from the calculated curve. If the ^{142}Nd was formed by 1% of p-process isotopes, it should fall close to the curve.

^{146,147}Sm–^{142,143}Nd isochrons. The ^{147}Sm–^{143}Nd isotopic compositions of the CAIs are shown in Extended Data Fig. 7a. We obtain an absolute ^{147}Sm–^{143}Nd age of 4,519 ± 140 Myr (MSWD = 0.77, initial ^{143}Nd/^{144}Nd = 0.50675 ± 0.00020) for all CAI fractions using a half-life value for ^{147}Sm of (6.539 ± 0.061) × 10^{-12} yr^{-1} (ref. 38). The initial ^{143}Nd/^{144}Nd is in agreement with previous determinations of the initial composition of ^{143}Nd/^{144}Nd in the Solar System of 0.50669 ± 0.00007 (ref. 27). If we calculate individual internal CAI isochrons, we find the most precise internal age for NWA 6991 of 4,523 ± 150 Myr (MSWD = 1.7, initial ^{143}Nd/^{144}Nd = 0.506 73 ± 0.00021). Our ^{147}Sm–^{143}Nd isochron ages are less precise than the Allende CAI age of 4,560 ± 34 Myr (ref. 18). A larger dispersion may come from the fact that we include four different CAIs from three different meteorites with potentially various evolution and metamorphic histories. Our mineral fractions have a limited range of Sm/Nd ratios in comparison to data presented in ref. 18. The melilite of NWA 2364 and melilite-residue of NWA 6991 with the lowest Sm/Nd ratio were too small for precise ^{142}Nd/^{144}Nd analysis and thus spiked for ^{143}Nd/^{144}Nd analysis.

In the ^{144}Sm/^{144}Nd versus ^{142}Nd/^{144}Nd diagram (Extended Data Fig. 7b), the slope of the best-fit line gives the ^{146}Sm/^{144}Sm ratio at the time of isotopic closure. When data obtained on the four CAIs from Allende, NWA 6991 and NWA 2364 are plotted together, they yield a ^{146}Sm/^{144}Sm ratio of 0.0073 ± 0.0022 (MSWD = 3.3) (Fig. 1). This ratio is indistinguishable (within errors) from the value of 0.0083 ± 0.0004 defined from the study of the Allende Al3S4 CAI[18].

In conclusion, the initial ^{146}Sm abundance deduced from CAI isochrons is inconsistent with the ^{146}Sm/^{144}Sm ratio obtained from the initial eucrite isochron calculated back to the age of CAIs using a half-life of 68 Myr (ref. 7). Instead, our

result and those of ref. 18 support the use of a ^{146}Sm half-life of 103 Myr (ref. 39). Having a good estimate of the ^{146}Sm half-life is essential for using this short-lived chronometer. As shown in Extended Data Fig. 8, such variation in the ^{146}Sm half-life produces age differences of up to 150 Myr for Hadean rocks.

Influence of CAIs on the bulk whole-rock carbonaceous chondrite Sm isotope compositions. The abundance of CAIs varies among chondrite groups, and CV chondrites contain on average about 3 vol% CAIs[40]. In CM chondrites, the proportion of CAIs is lower than in CV chondrites, and bulk samples are also characterized by lower deficits in ^{144}Sm (refs 3, 21). When we compare the measured ^{144}Sm negative anomalies measured in CAIs (this study) with enstatite, ordinary and carbonaceous whole-rock chondrites (this study and refs 3, 20) (Extended Data Fig. 9), we find that a volume abundance of CAIs in carbonaceous chondrites of approximately 3%–5% can explain the anomalies found in bulk CV3 (and CM2) chondrites, whereas enstatite chondrites and ordinary chondrites do not have any ^{144}Sm anomalies. However, the large deficit of ^{144}Sm in the Orgueil meteorite (CI chondrite, $\mu^{144}\mathrm{Sm} = -103 \pm 46$ p.p.m., ref. 3) cannot be explained by the presence of CAIs because the abundance of CAIs in CI chondrites is lower than 0.01% (ref. 40). Therefore, ^{144}Sm deficits are inherent to the matrix of CI chondrites instead of CAIs in CV and CM chondrites. This suggests that there are p-process deficits in all carbonaceous chondrite groups, hosted within the matrix in CI chondrites or within CAIs in other carbonaceous chondrite groups.

Conversely, CAIs have s-process deficits and r-process excesses, whereas the bulk rock isotope compositions tend towards a component that has an opposite signature, and that could be similar to the FUN inclusion EK1-4-1 (refs 41, 42), which display large excesses in r-process isotopes (Extended Data Fig. 5). Deficits in ^{144}Sm are carried by CAIs in CV chondrites, whereas deficits in ^{142}Nd are carried within the matrix of chondrites, and are the most extreme in carbonaceous chondrites.

The CAIs measured in this study have ^{147}Sm/^{144}Nd ratios between 0.1755 and 0.2405. Adding 3%–5% CAIs would increase the ^{147}Sm/^{144}Nd ratio of the CV bulk chondrites to 0.198. Literature ^{147}Sm–^{143}Nd data on Allende were reported in the supporting information of ref. 4. Measured Sm/Nd ratios for CV bulk rocks range from 0.1829 (ref. 35) to 0.2262 (ref. 43). These two extreme values were measured for very small Allende samples (90 mg and 0.6 mg, respectively). The dissolution of Allende bulk-rock chips of several hundreds of milligrams to 1 g gives values closer to the average chondritic ratio of 0.1960 (ref. 8). Five CV3 whole-rock chondrites were previously measured[27] to have an average ^{147}Sm/^{144}Nd ratio of 0.1955 ± 0.0058 (2 s.d.).

31. Krot, A. N., MacPherson, G. J., Ulyanov, A. A. & Petaev, M. I. Fine-grained, spinel-rich inclusions from the reduced CV chondrites Efremovka and Leoville: I. Mineralogy, petrology, and bulk chemistry. *Meteorit. Planet. Sci*. **39,** 1517–1553 (2004).
32. Bouvier, A., Brennecka, G. A. & Wadhwa, M. Absolute chronology of the first solids in the solar system. In *Formation of the First Solids in the Solar System* abstr. 9054 (2011).
33. Boyet, M. & Carlson, R. W. A highly depleted moon or a non-magma ocean origin for the lunar crust? *Earth Planet. Sci. Lett.* **262,** 505–516 (2007).
34. Marti, T. & Graf, T. Cosmic-ray exposure history of ordinary chondrites. *Annu. Rev. Earth Planet. Sci.* **20,** 221–243 (1992).
35. Rankenburg, K., Brandon, A. D. & Neal, C. R. Neodymium isotope evidence for a chondritic composition of the Moon. *Science* **312,** 1369–1372 (2006).
36. Rauscher, T. *et al.* Constraining the astrophysical origin of the p-nuclei through nuclear physics and meteoritic data. *Rep. Prog. Phys.* **76,** 066201 (2013).
37. Anders, E. & Grevesse, N. Abundances of the elements: meteoritic and solar. *Geochim. Cosmochim. Acta* **53,** 197–214 (1989).
38. Begemann, F. *et al.* Call for an improved set of decay constants for geochronological use. *Geochim. Cosmochim. Acta* **65,** 111–121 (2001).
39. Meissner, F., Schmidt-Ott, W. D. & Ziegeler, L. Half-life and α-ray energy of ^{146}Sm. *Z. Phys. A* **327,** 171–174 (1987).
40. Hezel, D. C., Russell, S. S., Ross, A. J. & Kearsley, A. T. Modal abundances of CAIs: implications for bulk chondrite element abundances and fractionations. *Meteorit. Planet. Sci.* **43,** 1879–1894 (2008).
41. McCulloch, M. T. & Wasserburg, G. J. Barium and neodymium isotopic anomalies in the Allende meteorite. *Astrophys. J.* **220,** L15–L19 (1978).
42. McCulloch, M. T. & Wasserburg, G. J. More anomalies from the Allende meteorite: samarium. *Geophys. Res. Lett.* **5,** 599–602 (1978).
43. Amelin, Y. & Rotenberg, E. Sm-Nd systematics of chondrites. *Earth Planet. Sci. Lett.* **223,** 267–282 (2004).
44. Barrat, J. A. *et al.* Geochemistry of CI chondrites: major and trace elements, and Cu and Zn Isotopes. *Geochim. Cosmochim. Acta* **83,** 79–92 (2012).

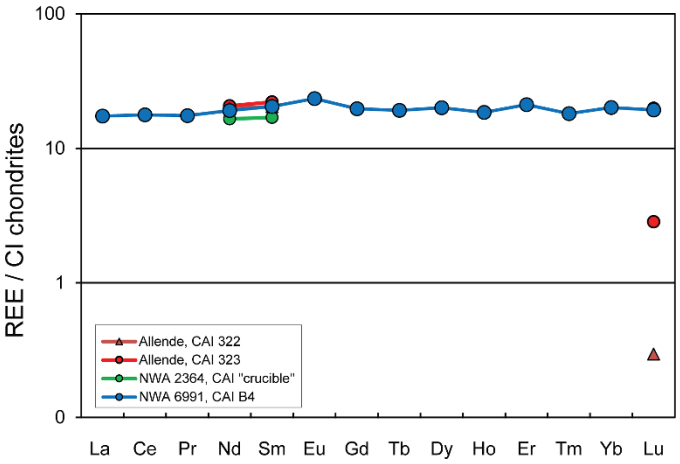

Extended Data Figure 1 | CI-normalized REE abundances in the four individual CAIs. CI average composition is from ref. 44. See Extended Data Table 1 for elemental concentrations.

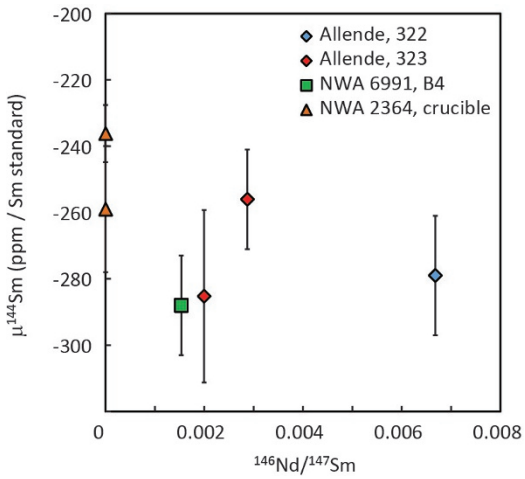

Extended Data Figure 2 | ^{146}Nd/^{147}Sm versus μ^{144}Sm from Allende 322 and 323, NWA 2364 and NWA 6991 bulk CAIs. The deviations are given in parts per million of ^{144}Sm/^{152}Sm ratios measured for samples compared to the average of measured Sm isotopic standards. Error bars represent internal errors (2 s.e.) for individual measurements. There is no correlation between the abundance of Nd within the Sm cuts with μ^{144}Sm compositions in individual CAIs. See Supplementary Tables 1–3 for isotopic data.

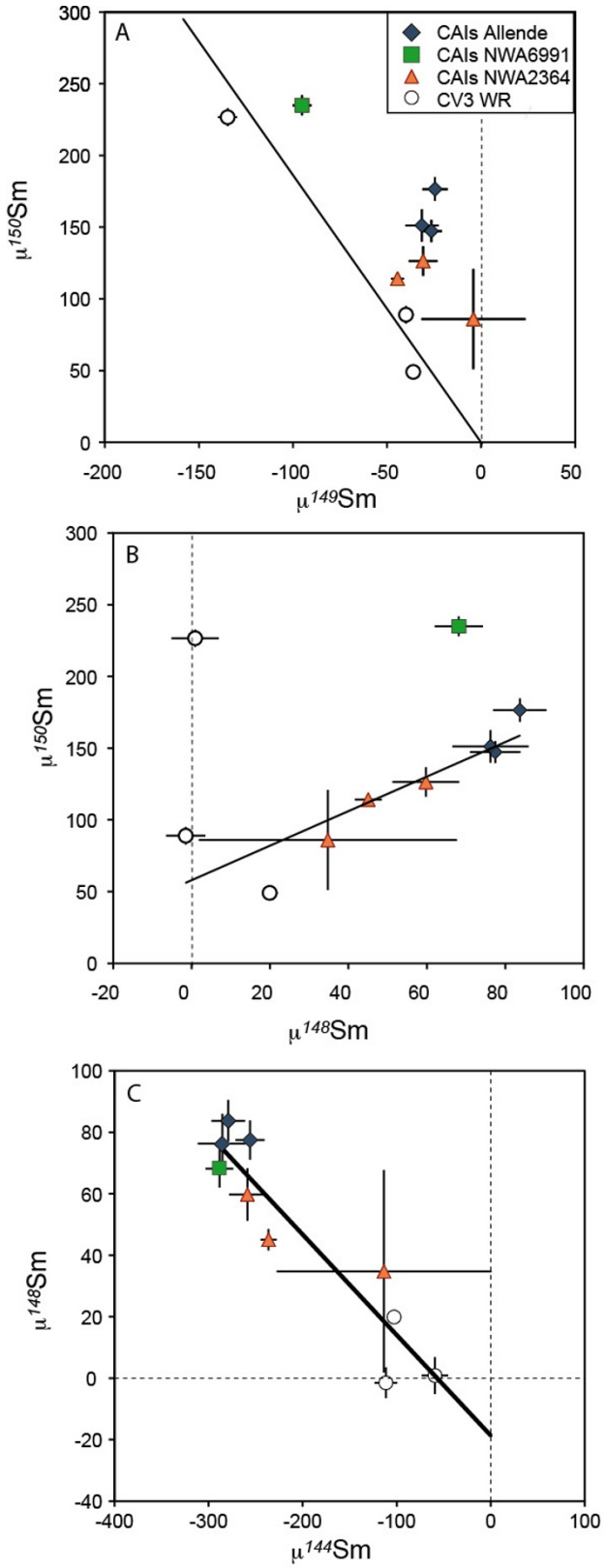

Extended Data Figure 3 | Sm isotopic ratios of CAIs and CV3 chondrites. Data for CV3 chondrites is from ref. 3. WR, whole rocks. Error bars indicate internal errors (2 s.e.) on individual measurements and black lines are best-fit lines.

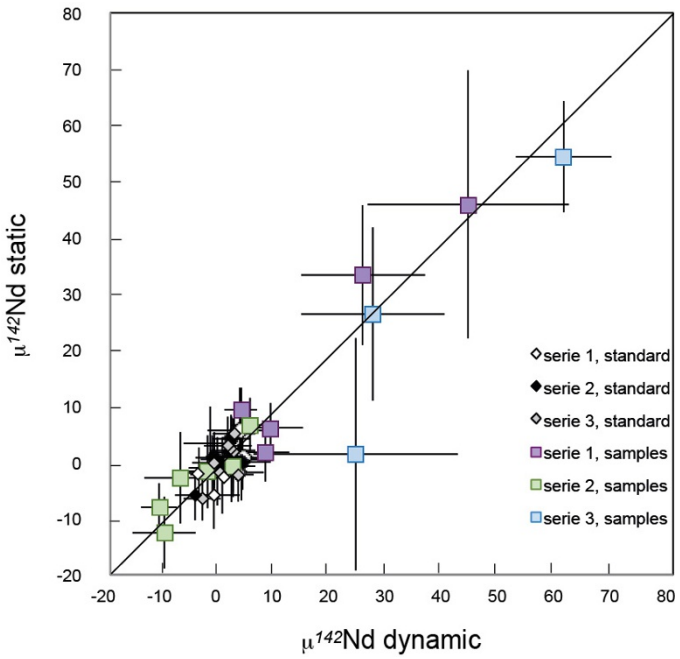

Extended Data Figure 4 | Deviation of $^{142}Nd/^{144}Nd$ ratios relative to the JNdi-1 standard measured in dynamic and static modes. Deviations are given in parts per million. For static mode, the Faraday cup for line 1 was centred at an atomic mass of 145. Error bars indicate internal errors (2 s.e.) on individual measurements and the black line indicates a slope of one.

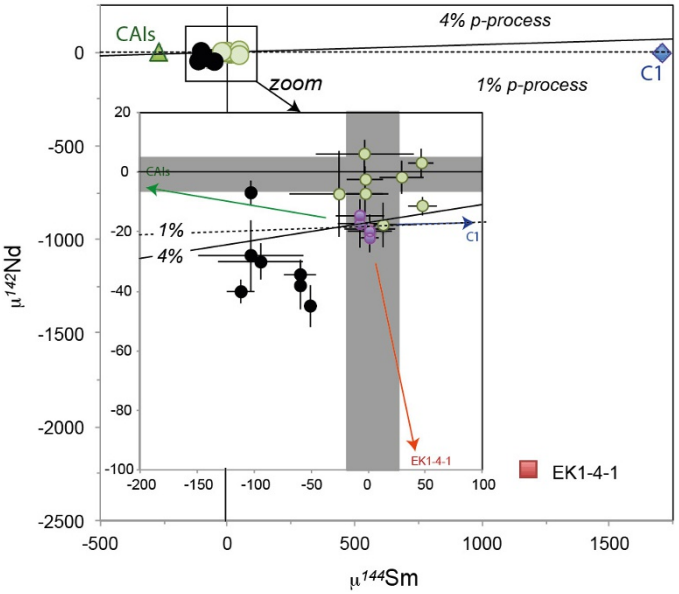

Extended Data Figure 5 | $^{144}Sm/^{152}Sm$ versus $^{142}Nd/^{144}Nd$ expressed in μ notation. Chondrite data (black circles, carbonaceous chondrites; purple circles, ordinary chondrites; green circles, enstatite chondrites) are from this study and refs 3 and 4. CAIs, FUN inclusions (EK1-4-1 and C1; refs 41, 42) and chondrite $^{142}Nd/^{144}Nd$ ratios are corrected for radiogenic decay of ^{142}Nd over the age of the Solar System. Gray boxes show 2σ external reproducibility obtained on the standard. Solid and dotted lines correspond to p-process contributions for ^{142}Nd of 4% and 1%, respectively. The complementary part is formed by s-processes. Our data show that there is no correlation between $\mu^{144}Sm$ and $\mu^{142}Nd$, in contrast to previous suggestions[4].Error bars indicate internal errors (2 s.e.) on individual measurements when larger than symbols and available.

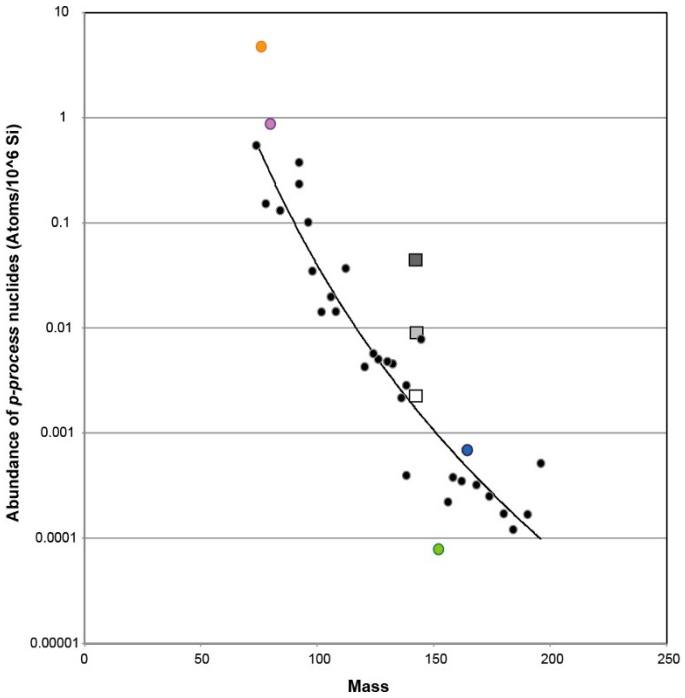

Extended Data Figure 6 | Abundance of p-process nuclides versus mass. Black dots show isotopes formed by p-processes only; coloured dots show isotopes formed partly by p-process and partly by s-processes (orange, ^{76}Se; purple, ^{80}Kr; green, ^{152}Gd; blue, ^{164}Er). Model abundances of ^{142}Nd are represented by the squares coloured in dark grey for a 20% p-process contribution, light grey for 4% and white for 1%. The black line is the best-fit line.

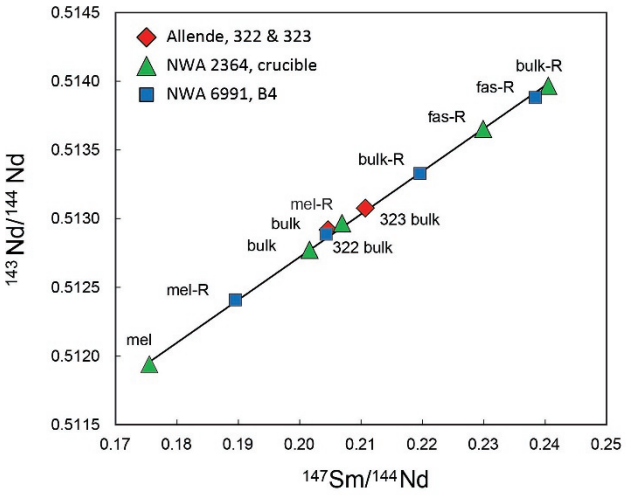

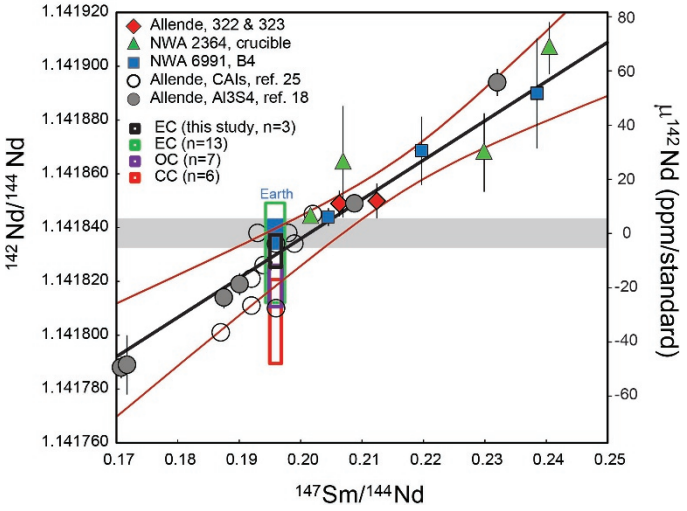

Extended Data Figure 7 | Sm–Nd internal isochrons of CAIs from Allende, NWA 2364 and NWA 6991. a, ^{147}Sm–^{143}Nd internal isochron. By combining all the CAI fractions together and fitting the data to a straight line, we determine the ^{147}Sm–^{143}Nd age to be 4,526 ± 150 Myr (MSWD = 1.2, initial $^{143}Nd/^{144}Nd = 0.50673 \pm 0.00021$). R, residue after leaching; fas, fassaite; mel, melilite. **b**, The black line represents the ^{146}Sm–^{142}Nd internal isochron of CAIs from Allende 322 and 323, NWA 2364 and NWA 6991; red lines indicate the 95% confidence interval. ^{146}Sm–^{142}Nd systematics of Allende bulk and mineral separates (Al3S4)[18] and Allende bulk CAIs[25] are shown for comparison (error bars are not shown because individual analytical errors were not provided). The blue rectangle represents the composition of modern Earth's mantle, as represented by our long-term measurements of the JNdi-1 standard ($^{142}Nd/^{144}Nd = 1.141838 \pm 0.000006$; by definition, $\mu^{142}Nd = 0$) with $^{147}Sm/^{144}Nd = 0.1960$, which is within the error of the regression for CAIs from this study. The other rectangles represent the averages for $\mu^{142}Nd$ with 2 s.d. given below with values of -7 ± 6 p.p.m. for enstatite chondrites (EC; black, value from this study, $n = 3$), -6 ± 18 p.p.m. for enstatite chondrites (green, $n = 14$), -18 ± 6 p.p.m. for ordinary chondrites (OC; purple, $n = 5$) and -34 ± 18 p.p.m. for carbonaceous chondrites (CC; red, $n = 8$), all normalized at $^{147}Sm/^{144}Nd = 0.1960$ (the widths of the rectangles for $^{147}Sm/^{144}Nd$ are exaggerated for clarity).

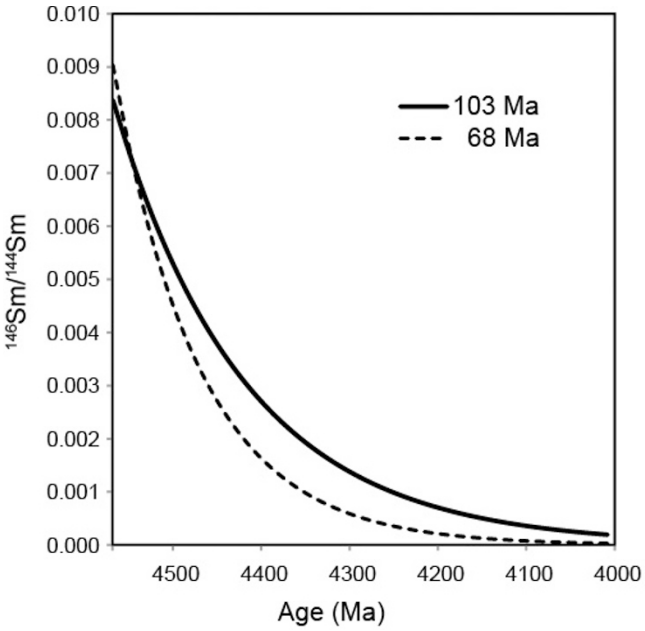

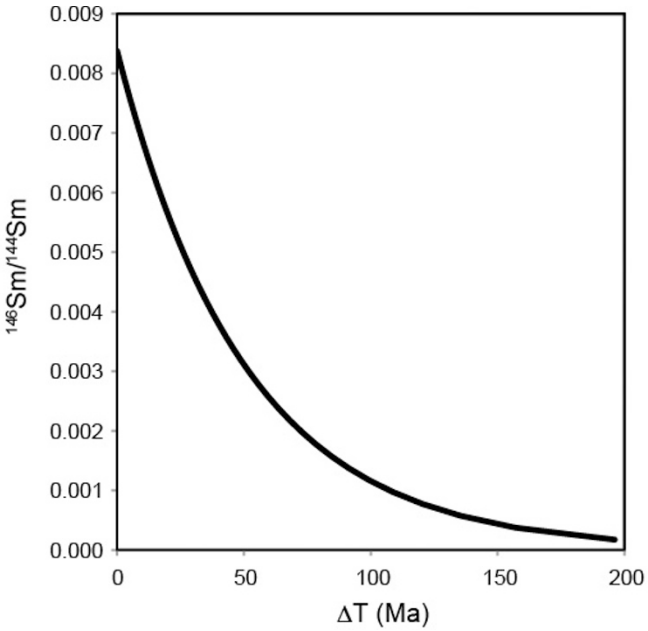

Extended Data Figure 8 | Evolution of the $^{146}Sm/^{144}Sm$ ratio. Left, $^{146}Sm/^{144}Sm$ ratio as a function of age using the two proposed decay constants for the short-lived ^{146}Sm radionuclide. The two curves intersect at $^{146}Sm/^{144}Sm = 0.0073$ and 4,546 Ma—the values defined from eucrite internal isochron of Binda in ref. 8. For objects formed after 4,546 Ma ago, ages are younger using the 103-Ma half-life value. Right, time difference ΔT obtained using the two decay constants proposed for ^{146}Sm. Ma, millions of years.

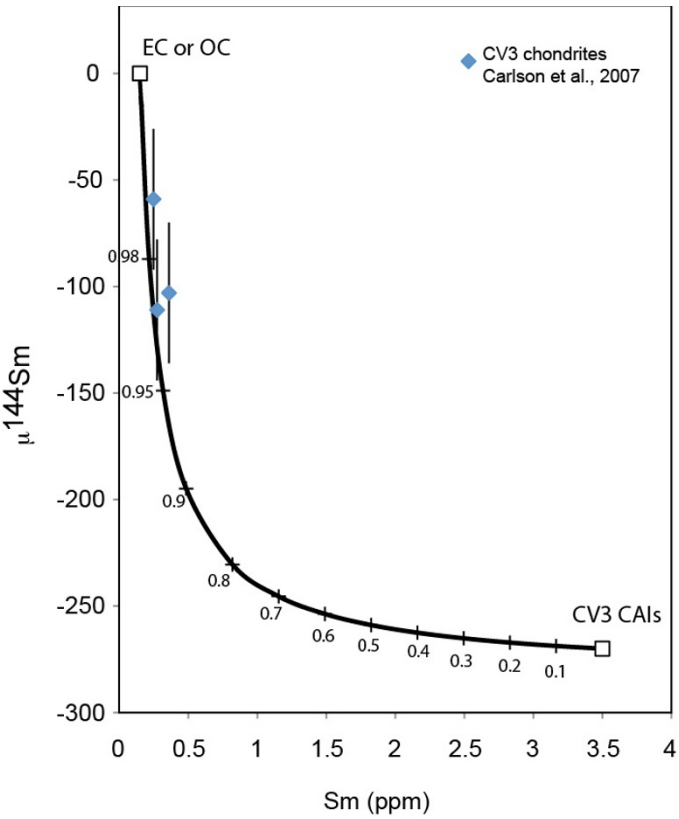

Extended Data Figure 9 | Mixing model (black line) between CV3 CAIs (^{144}Sm abundance measured in this study) and matrix (enstatite chondrite (EC) and ordinary chondrite (OC) whole-rock meteorites without a ^{144}Sm anomaly) (open squares). ^{144}Sm anomalies measured in CV3 chondrites (blue symbols) correspond to 1%–3% CAI volume abundances in the mixing model[3,20]. The numbers on the line indicate the proportion of matrix-component end-member relative to CAI end-member. Error bars (2 s.e.) are for individual measurements of whole-rock CV3 chondrite meteorites.

Extended Data Table 1 | Concentrations of REEs in individual bulk and unleached CAIs

Method	Samples	La	Ce	Pr	Nd	Sm	Eu	Gd	Tb	Dy	Ho	Er	Tm	Yb	Lu
ID	Allende, 322	-	-	-	9.00	3.02	-	-	-	-	-	-	-	-	0.007
ID	Allende, 323	-	-	-	9.47	3.27	-	-	-	-	-	-	-	-	0.070
ID	NWA 2364, crucible	-	-	-	7.56	2.51	-	-	-	-	-	-	-	-	0.490
ICPMS	NWA 6991, B4	4.12	10.9	1.62	8.73	3.03	1.32	3.92	0.691	4.93	1.01	3.38	0.448	3.25	0.475

Concentrations are given in parts per million and were measured by quadrupole ICPMS or isotopic dilution (ID) methods by MC-ICPMS.